Evaluation of seismic response of bridge piers by surface mounted optical fiber sensors

S.A. Bassam, A. G. Tennant, and F. Ansari
University of Illinois at Chicago, Chicago, Illinois, USA

ABSTRACT: Recent advances in design of bridges in seismic zones have resulted in design and construction of more ductile piers. Although, this approach produces more effective design for safeguard against brittle failure, their behavior under actual seismic loading conditions needs to be assessed. The study reported here describes development of multiplexed optical fiber sensors systems for real time detection of seismic response in such piers. The sensors are capable of measuring displacement and frequency response over desired gauge lengths. Evaluation of the sensors involved shaking table experiments on single column bents subjected to actual near fault zone seismic loads. This paper describes development of the FBG based sensors system and the experimental results.

1 INTRODUCTION

A number of essential application areas in civil structures such as post seismic and disaster monitoring have received very little attention. However, many of the novel sensors that have been developed over the past decade have the potential for effective post hazard evaluation of the structures (Ansari, 2005). One objective of the project described in this paper was to investigate the performance of bridge piers which are designed based on Caltran provisions in near-fault earthquakes by use of fiber optic sensors.

Characteristics of near-fault ground motions are peculiar compared to far-field ground motions, which nearly all design criteria are based on. Current simple amplification of far-field design spectra in some codes may not necessarily be adequate to account for the near-field effect.

The California State Highway system has more than 12000 bridges in its inventory and an additional 11500 city and country bridges (Caltrans fact sheet, 2001). A site-specific process which is required for bridges located near active fault in Caltrans Seismic Design Code (SDC) can be costly, long, and non-standard. The purpose of this study was to investigate near-fault ground motion effects on typical Caltrans columns. The ultimate goal is to develop practical and proven bridge design guidelines that incorporate the effects of near-fault ground motions.

Another objective was the dynamic verification of performance through shaketable testing. To meet these objectives, a column, designated ETN, was the subject of the test. The design of ETN was based on current Caltrans Bridge Design Specifications (v 1.3, 2004) near-fault seismic design guidelines. This column was subjected to the Rinaldi ground motion. The Rinaldi record was captured from 1994 Northridge earthquake and included typical near-fault motion characteristics. Special Fiber Bragg Grating (FBG) displacement sensors were designed and used to measure the dynamic characteristics of the column. The experiments were performed at the University of Nevada, Reno shaketable test facility under a payload project funded by the National Science Foundation.

2 SPECIMEN DESIGN

The column was reinforced with 22 12.7mm diameter longitudinal bars (f_y=*486 MPa*, and 6.35mm diameter spiral reinforcement (f_y=*424 MPa*) spaced at 25.4 mm. The axial load ratio was 8%.

A length scale of 1/3 relative to the full scale prototype was chosen based on the test set-up capacity. This scale ensured the column to be tested to complete failure. Rigid footings were designed, constructed and post tensioned to the shaketable deck. Details are given in Table 1.

3 TEST SETUP AND PROCEDURE

3.1 *Test Setup*

One of the shaketables at the University of Nevada, Reno was used to test the column. The test setup is shown in Figure 1. The inertial mass and the column axial loads were applied through separate systems. The weights for the inertial force were placed off the table on a four hinge frame shown on the right side of the column in Figure 1. Concrete blocks were placed on the mass rig and were attached to the top of the specimen by a very stiff link with an internal load cell to record the load transferred. The column axial force was applied by a pair of hydraulic jacks connected to a pair of pre-tensioned bars on the top of the column. The pre-tensioned bars were tied into the base of the footing. The effect of the axial load system on the column performance was studied and shown to represent the axial component typical in bridge systems. An accumulator was placed in the hydraulic line to minimize variation of axial force.

Table 1. Column design details

scale	30%
column height	2.76 m
column diameter	36 cm
axial load	276 KN
concrete design strength	29.8 Mpa
longitudinal steel ratio	3%
longitudinal bars	22 No. 4 bars
longitudinal bar yield stress	486 Mpa
transverse steel ratio	1.54%
confinement type	6.35 mm-diameter hoops
confinement yield stress	424 Mpa
pitch	25.4 mm
concrete cover	1.9 cm
subjected ground motion	Rinaldi (Northridge)
design criteria	Caltrans SDC Ver. 1.3 (2004)

Fiber Bragg Grating (FBG) sensors encapsulated in a composite material and backed with polyimide sheets and then mounted on the column surface were used for measurement of displacements, curvatures and other dynamic parameters such as vibration frequency and damping ratios. The gauge length of the sensors was 100mm.

Four pairs of FBG sensors were installed along the bottom surface of the column. The displacement sensors were installed directly to the column by use of epoxy. Sensor location and numberings are shown in Figure 2a, b, and c. The horizontal displacement was also measured at the top of the column by use of a wire displacement transducer. The inertial forces were measured using a load cell and an accelerometer placed on the loading block.

3.2 *Test Procedure*

A recorded event, in this case the Northridge, California earthquake of January 17, 1994 was used. The earthquake caused the failure of six bridges and irreparable damage to four others.

A quasi-static testing approach was used which consisted of increasing the exciting acceleration amplitudes by multiplying a scalar of the recorded Rinaldi ground accelerations. A total of ten steps were used starting with 0.05 x full Rinaldi scale and ending with 1.35 x full Rinaldi scale. Table 2 shows the peak acceleration and test scale for each run of the test.

Figure 1. Shaketable, specimen, and mass rig test setup

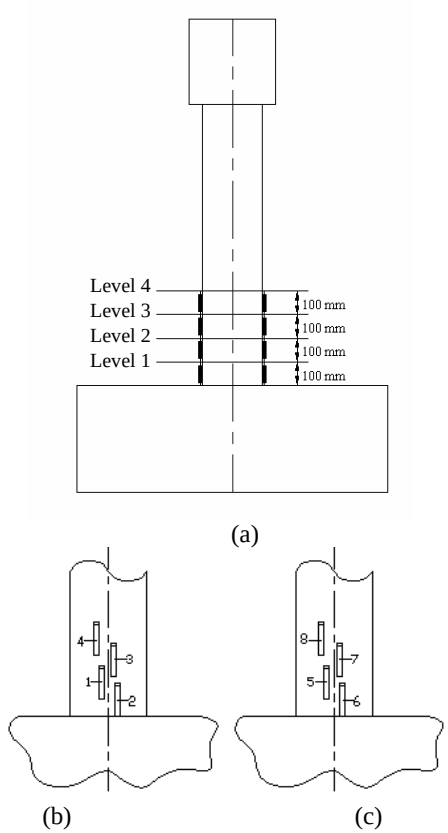

Figure 2. Sensor arrangement. a- sensors location. b- sensor numbering in column front view. c- sensor numbering in column back view

Table2. Input earthquake amplitudes

Event	x Rinaldi	PGA (g)
1	0.05	0.04
2	0.2	0.17
3	0.3	0.25
4	0.45	0.38
5	0.6	0.5
6	0.75	0.63
7	0.9	0.75
8	1.05	0.88
9	1.2	1.01
10	1.35	1.13

4 EXPERIMENTAL RESULTS

Typical time history of the displacements measured by sensor No. 8 is shown in Figure 3. Most of the sensors could survive after applying the full scale earthquake load on the column which shows good reliability of the designed sensors.

4.1 *Moment curvature analysis*

Curvatures are more sensitive to local damage than other parameters. Knowing the curvatures, one can directly calculate the bending stiffness EI, the reduction in which is commonly believed to be a significant indicator of damage:

$$EI = \frac{M}{\phi} \tag{1}$$

where E is the concrete modulus of elasticity, I is the section moment of inertia, M is the moment and ϕ is the curvature. Curvature could be obtained using the following relationship:

$$\phi = \frac{\varepsilon_2 - \varepsilon_1}{d} \tag{2}$$

where d is the diameter of the column, and ε_1 and ε_2 are the strains on the opposite sides of the column measured through the FBG sensors.

For each event, moment curvature hysteresis diagrams at different levels were calculated by obtaining the force at the top of column from the force link and multiplying that by the distance to the desired level. A typical moment curvature hysteresis diagram is shown in Figure 4. For each event, four moment curvature diagrams corresponding to four different levels could be obtained. The maximum moment in each of these diagrams and the corresponding curvature were recorded to obtain the global moment curvature envelope for each level. The results are displayed in Figure 5.

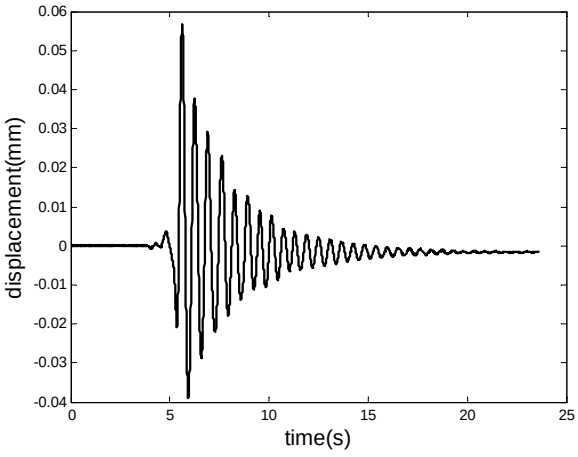

(a)

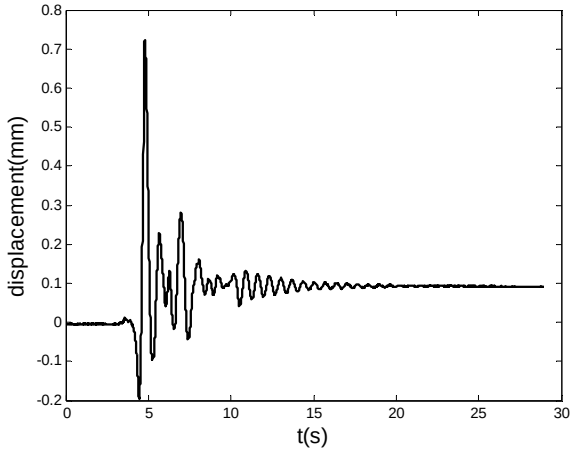

(b)

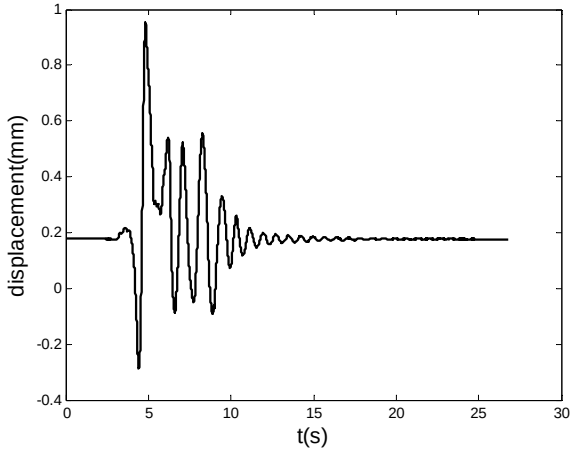

(c)

Figure 3. Typical time history of the crack opening displacements measured at the location of sensor No. 8. a- Time history at event 1 (A_{max}=0.04g) b- Time history at event 5 (A_{max}=0.5g) c- Time history at event 8 (A_{max}=1.05 g)

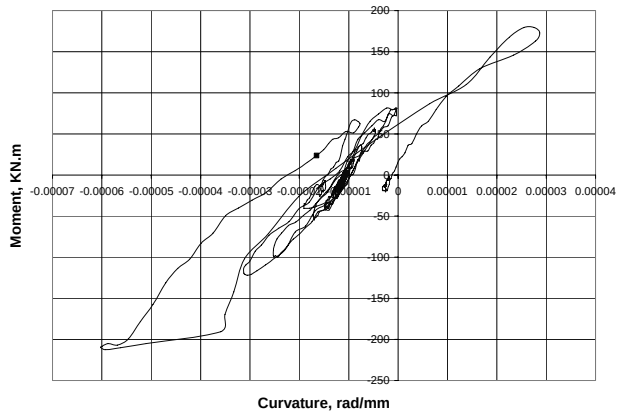

Figure 4. Typical Moment-curvature hysteresis diagram at event 6, level 1

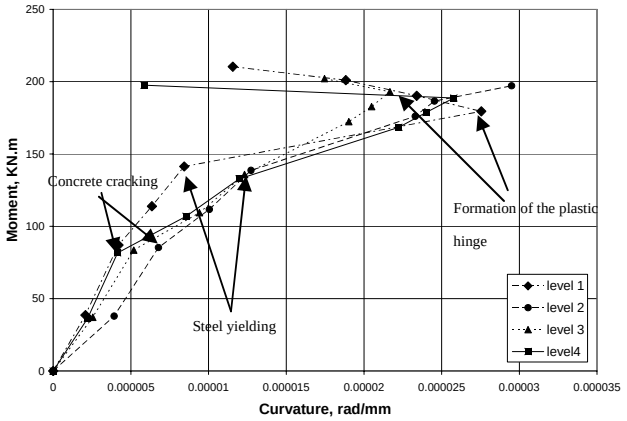

Figure 5. Moment curvature envelope diagrams

The moment-curvature envelope in figure 5 shows some interesting results. Change of slope for all levels happens in several locations. First significant change of slope happens at the second event (corresponding to 0.20 full scale Rinaldi, $A_{max}=0.17g$). This change of slope shows that the concrete cracks happened at this event which caused nonlinearity in the behavior of the column. Second significant change of slope can be observed at the 4th event (corresponding to 0.45 full scale Rinaldi, $A_{max}=0.38g$). This change shows the yielding of the reinforcement which induces more nonlinearity in the structural behavior. Finally, except for event 2, all other events show a significant reduction in the measured curvature after the 6th event (corresponding to 0.75 full scale Rinaldi, $A_{max}=0.63g$). Reduction in curvature is due to the reduction in the strains measured by the FBG sensors which is caused by the formation of the plastic hinge. When the plastic hinge is formed, the strain energy stored in the structure will be released and the column displacements will be mainly due to the rigid body motion around the hinge. However, at the place of the hinge, the strains would still increase since all the damage will be localized at that point. Figure 5 clearly shows this phenomenon in which all the sensors show a significant reduction in the measured strain except the sensors located at level 2 (150 mm above the base of the column). Visual investigation verified an extensive damage localized at this location during this event. Figure 6 shows the spalling of concrete at the location of level 2 following this event.

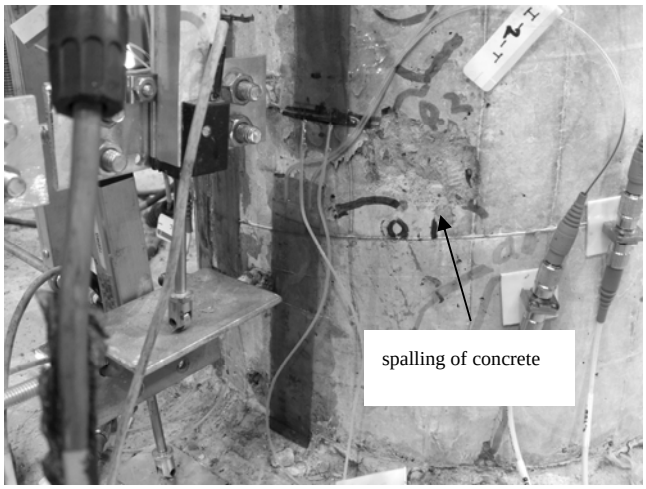

Figure 6. Spalling of concrete at level 2 (150 mm above the base) after event 6 (0.63g PGA)

It is interesting to note that although the maximum moment happens at the base of the column, the plastic hinge is formed in an upper level. This might be due to the effect of concrete confinement which prevents the cracks to develop at the base of the structure. Detection of the plastic hinge provides a tool in structural health monitoring in seismic zones.

4.2 *Spectral response of the column*

Depending on the location and severity of damage, modal parameters, especially natural frequencies and damping ratios will change in the structure. The main advantage of using vibration monitoring as a damage indicator tool is due to its simplicity and economy. Any localized damage in a structure reduces the stiffness and increase the damping ratio in the structure. Reduction in stiffness is associated with decrease in the natural frequencies. Several researchers (Adams et al 1978, Cawley et al 1979, and Yuen 1985) have identified and predicted damage by noting the change in natural frequencies. Due to the high sampling frequency and noiseless nature of the FBG sensors, they are ideal for measuring the vibration frequency of the structure.

Power Spectral Density (PSD) of each sensor was calculated via Welch method in each event. In order to eliminate the interference of the frequency content of the loading with the fundamental frequency of the structure, the loading portion of the signal was removed and only free vibration portion of the signal

was used in calculation of PSD. Figures 7a-c show a typical full signal, the free-vibration portion of the signal and the corresponding frequency response of the signal obtained from sensor 3 at event 6.

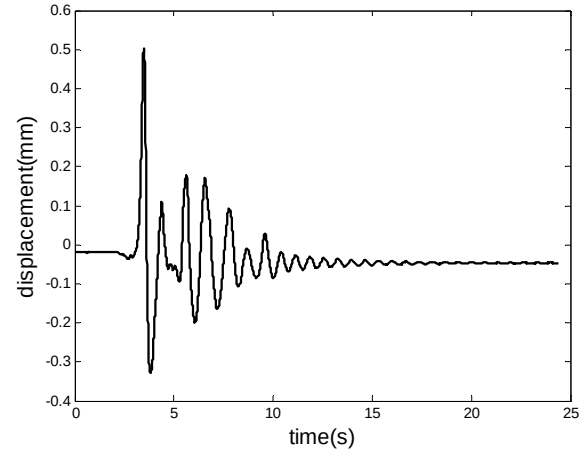

(a)

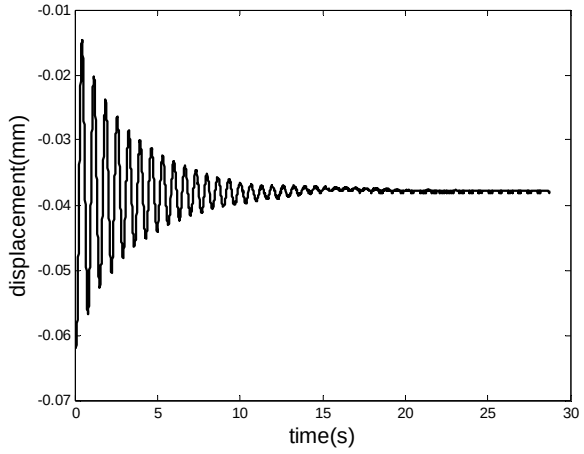

(b)

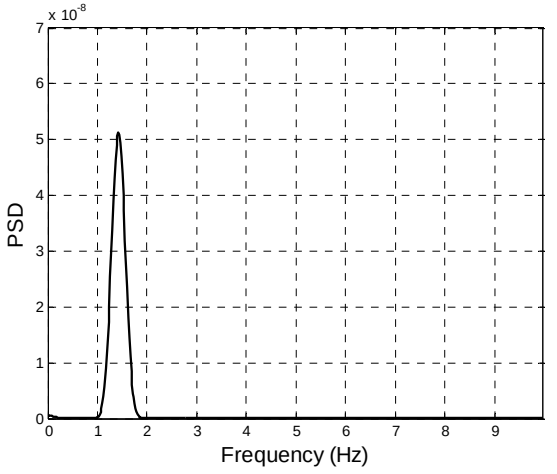

(c)

Figure 7. a-Full event signal b-Free vibration portion of the signal c-Power Spectral Density

Analysis of the signals indicated that all the sensor signals result in exactly the same value for the fundamental frequency of the column in each event. However, as shown in Figure 8, the fundamental frequency of the column decreases for increasing levels of damage for the events studied. Results for all events are shown in Figure 8.

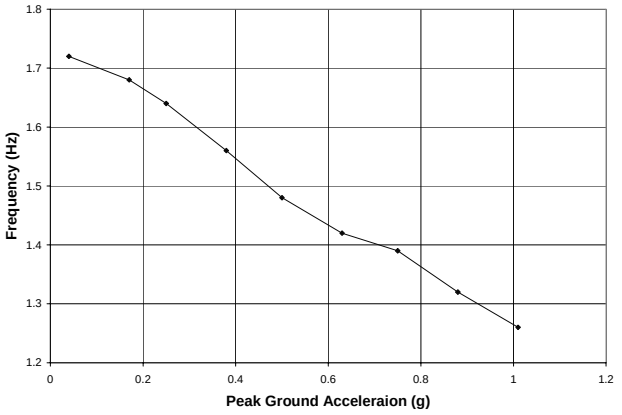

Figure 8. Amplitude dependence of the resonance frequency for different loading steps

4.3 *Measured damping*

Damping was calculated by fitting an exponential function to the peaks of the sensors free vibration response (log decrement procedure). As predicted, damping ratios increase in each event commensurate with increasing levels of damage in the structure. The results are shown in Figure 9.

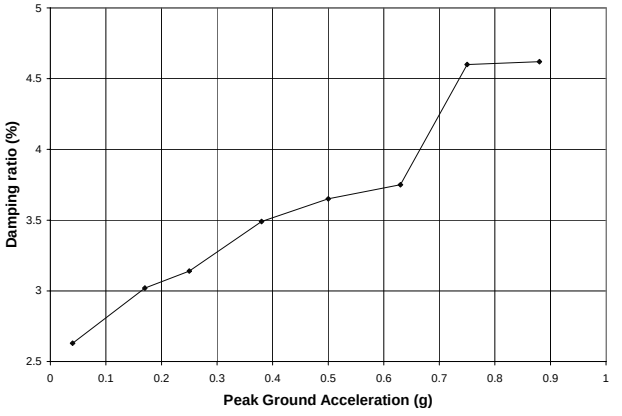

Figure 9. amplitude dependence of the damping ratios for different loading steps

As shown in Figure 9, event 7 shows a significant jump in the damping ratio amplitude. This coincides with the formation of the plastic moment hinge as indicated. It seems that the change in damping ratio is more sensitive to the damage than the shift in frequency. However, more experimentation is necessary to fully verify this.

Results presented in this article were based on testing of one column. More tests are required to verify the applicability of the presented FBG sensors in post hazard evaluation of the structures. A large scale bridge will be tested at the University of Nevada, Reno in near future The test will involve three shaketables for testing of the structure and verification of the health monitoring and post hazard evaluation capabilities of the sensors.

5 CONCLUSION

Following general conclusions may be drawn from the results:

1- The fiber optic sensors used in this study could survive even following the full scale seismic loads experienced by the column. Considering their high resolutions and high resistance in harsh environmental conditions, using these types of sensors is recommended for the health monitoring applications where high reliability of the measuring sensor is required.

2- Moment curvature diagrams obtained from the surface mounted FBG sensors could precisely detect the cracking of concrete, yielding of the steel and the formation of the plastic hinge. This is useful for deterministic post seismic evaluation of the structures.

3- Fiber optic sensors could obtain natural frequency of the column with great precision for use as a tool to measure the extent of the damage in the structure.

4- Increase in damping ratios obtained from the free vibration response of the column showed more sensitivity to the extent of the damage than the reduction in natural frequency.

ACKNOWLEDGEMENT

This project was made possible by the National Science Foundation grant number CMS-0523333. The financial support of the Photonics Technology Access Program (PTAP) for the design and acquisition of the special prototype fiber optic sensor interrogation unit is greatly appreciated. The shaketable experiments were conducted at the University of Nevada, Reno (UNR) as part of the NSF-NEES project under the direction of Prof. Saiid Saiidi. The post hazard monitoring of the column with fiber optic sensors was conducted in parallel with UNR's experiments. The cooperation of UNR researchers and staff with this work is greatly acknowledged.

REFERENCES

Adams, R. D., Cawley, P., Pye, C. J., Stone, B. J.1978. A vibration technique for non-destructively assessing the integrity of structures. *Journal of Mechanical Engineering and Science*. Vol. 20, No. 2. pp. 93-100.

Ansari, F.(ed.) 2005. *Sensing Issues in Civil Structural Health Monitoring*. the Netherlands: Springer publishing Co. 528 pp.

Caltran fact sheets 2001. http://www.dot.ca.gov/hq/paffairs/about/retrofit.htm

Caltrans 2004. Bridge Design Specifications. Technical Publications. www.dot.ca.gov/hq/esc/techpubs/. Section 8. pp. 8-1 to 8-58

Cawley, P., and Adams, R. D. 1979. The location of defects in structures from measurements of natural frequencies. *Journal of strain Analysis*. No. 4. pp. 49-57.

Yuen, M. M. F. 1985. A numerical study of the eigenparameters of a damaged cantilever. *Journal of Sound and Vibration*. No. 103. pp. 301-310.